- Technical Paper -

NUMERICAL SIMULATION OF PROPERTIES OF DRIED CONCRETE CONSIDERING INTERFACIAL TRANSION ZONE

Kota OGAWA[*1], Yoshihito YAMAMORO [*2], Ippei MARUYAMA [*3]

ABSTRACT

This paper described new insights on the influence of interfacial transition zone on drying shrinkage strain and compressive strength of concrete through numerical simulation. Using Rigid Body Spring network Model, analysis of drying shrinkage and compression test of drying concrete are performed considering long and short term model of ITZ. As a result, experimental trend is reproduced by using the proposed model. This reproducibility indicated that ITZ characteristics should be taken into account to simulate the shrinkage and strength of dried concrete simultaneously.

Keywords: inter facial transition zone, drying, shrinkage strain, compressive strength, crack

1. INTRODUCTION

Integrity of concrete structure through its service life should be required. For integrity evaluation process, it is necessary to evaluate the required performance at present and in future [1]. To predict structural performance of concrete in future, which is generally changing during its service life, it is important to elucidate the deterioration factors of concrete and to establish the fundamental knowledge of the aging concrete. Many studies have been reported about the factors visible and considered to be crucial, such as salt damage, frost damage, carbonation, and drying shrinkage crack. On the contrary, few studies have been reported about the impact of drying on both shrinkage and strength. But those have large impact on structural response to earthquakes [2].

Now, unknown factor of numerical modeling of concrete with regards to material performance concrete is in interfacial transition zone (ITZ). According to previous studies, concrete forms ITZ between aggregate and paste. It is generally considered that this ITZ is porous and strength and Young's modulus of ITZ are lower than that of normal cement paste or mortar region [3-5]. This porous region is produced in the concrete when it is fresh state and the aggregates capture rising bleeding water from bottom side. In matured state, the portlandite is precipitated much rather than normal mortar or paste region, because the bleeding water contains rich calcium ions which is the most rich ion in the pore solution of concrete [6]. This ITZ has strong impact on concrete property such as diffusion process [7], strength [8], and shrinkage behavior [9].

Based on these backgrounds, in the present contribution, we investigated an impact of ITZ on mechanical performance of concrete through numerical simulation to reproduce the drying shrinkage strain and compressive strength of dried concrete.

2. NUMERICAL MODEL

2.1 RBSM

Rigid Body Spring network Model (RBSM) was employed in this study. In RBSM, a continuum material is considered as an assembly of rigid particle elements interconnected by zero-size springs along their boundaries. In the present modeling, each interface between two rigid particles was divided into several triangles sharing the barycenter of the interfacial plane, with each triangle having three individual springs, one for a normal force and two for orthogonal tangential forces as it is shown in Fig. 1.

At the same time, the nonlinearity of normal and tangential springs can take into account the nonlinearity of the rotation behavior on the interfacial plane.

The nonlinearity and discrete behavior of the continuum material is emulated by cracks developing at the interfaces of the rigid particles. For this reason, crack patterns and the resultant nonlinear behavior of the target model are significantly affected when a mesh design is employed. To solve this problem, random geometry using Voronoi diagrams was applied

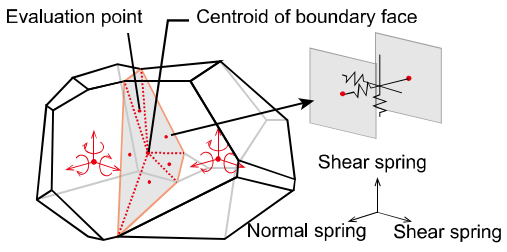

Fig. 1 Schematic of the elements in RBSM and springs connecting them

*1 Dept. of Environmental Eng. And Arch., Nagoya Univ.
*2 Assoc.Prof Dept. of Civil Engineering, Nagoya Univ., Dr.Eng
*3 Assoc.Prof Dept. of Environmental Eng. and Arch, Nagoya Univ., Dr.Eng

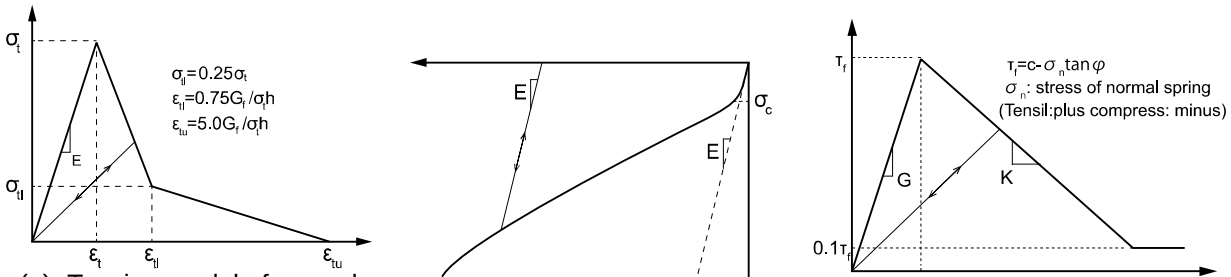

(a) Tension model of normal spring

(b)Compression model of normal spring

(c)Shear spring model

Fig. 2 Schematic of stress-strain relationships for mortar and aggregate springs.

Table 1 Physical properties of materials in the numerical analysis.

	Normal spring			
	Young's modulus E*(N/mm^2)	Tension strength Ft*(N/mm^2)	Fracture energy Gf*(N/m)	Compressive strength Fc*(N/mm^2)
Mortar	18	3.5	70	46.7
Aggregate	70	200	—	200
ITZ	—	—	7	46.7

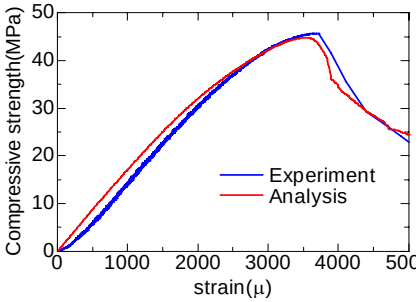

Fig. 3 Result from analysis of fitting mortar

Table 2 Applied values of springs in the numerical calculation (* is experiment and italic is analytic)

Normal spring				Shear spring			
Young's modulus E (N/mm^2)	Tension strength ft (N/mm^2)	Fracture energy G_f (N/m)	Compressive strength f_c (N/mm2)	Cohesion c (N/mm2)	Internal friction angle ϕ (degree)	Fracture criterion σ_b (N/mm^2)	$\eta=G/E(-)$ (G : Shear stiffness)
1.4E*	1.2Ft*	0.5Gf*	1.5Fc*	0.14Fc*	37	0.5Fc*	0.40

2.2 Modeling of concrete material

In this study, to represent the fracture behavior of drying concrete, three different phases are modelled namely, mortar springs between mortar elements, aggregates springs between aggregate elements, and ITZ spring between mortar and aggregate elements.

2.2.1 Modeling of mortar matrix and aggregate

Figure 2 shows schematic of stress-strain relationships for mortar and aggregate springs and Table 1 shows the material properties. For the mortar and aggregate springs, tensile behavior is modeled by a linier elastic up to tensile strength, followed by bilinear softening branch of 1/4 model based on a given tensile fracture energy. Compression behavior of mortar and aggregate springs is modeled by S-type curve derived a relationship between stress and volume under hydrostatic pressure conditions. This model will not collapse in compression. In case of shear spring, its behavior is defined by Mohr-Coulomb type criterion. The shear strength is decided by the stress of normal spring and is assumed to be constant when the normal stress is greater than σ_b in Fig.2(c)

2.2.2 Parameter of materials

Parameters for the constitutive laws are calibrated by conducting parametric study following the pioneer work of the proposed model [10]. For this process, uniaxial compression test of mortar is conducted [11]. The results were summarized in Table 2 and Fig. 3.

3. ANALYSIS OF DRING SHRINKAGE

3.1 Analysis object

Figure 4 shows the analysis object. Specimen with dimension ϕ50×100mm is target of the present numerical analysis. The detail of the experiment is shown in our previous paper [11]. Three dimensional mesh of the surface of the target specimen is shown in Fig. 4(a). The specimens are modeled as a two-phase model, such as mortar matrix and aggregates. Fig. 4(b) shows the distribution of aggregates in the target specimen and Fig. 4(c) shows a cross sectional plane of the target specimen for the clarity of the distribution of the aggregates. In this figure, the white color represents mortar elements, and the black color is corresponding to the aggregate elements. The size of coarse aggregate particles is set from 8mm to 20mm. In this model, based on the companion experiment, the total volume

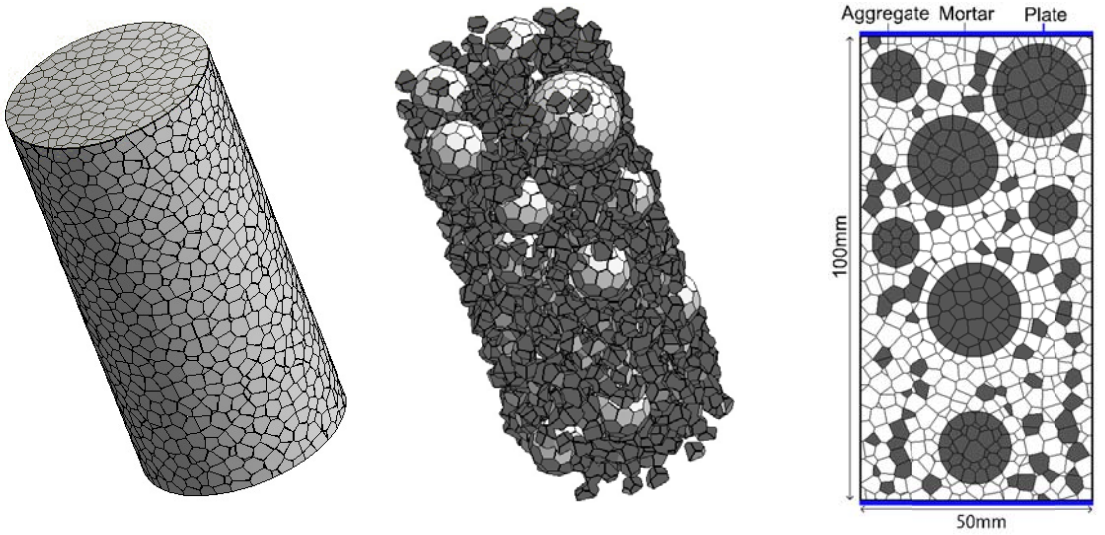

(a) Voronoi diagram of surface

(b) Three dimensional distribution of coarse aggregates

(c) Sectional plane (Plate elements are used only for loading calculation.)

Fig. 4 Mesh for the analysis

of coarse aggregate elements to the concrete specimen is about 32% according to the mixture proportion of the experiment. Average characteristic radius of each element is about 2 mm.

3.2 Analysis method

Shrinkage behavior of this specimen is attained by simulating the shrinkage of mortar and ITZ behavior. The shrinkage of mortar under different equilibrium drying conditions are based on our previous experiment [11] in Fig. 5, they are 900μ at 60% RH and 20 ºC, 1300μ at 20% RH and 20 ºC, and 1400μ at 60 ºC. For the drying process, 10μ-incremental shrinkage was applied to the mortar springs as equivalent nodal force. In this simulation, different thermal expansion of mortar and aggregate and the damage caused by temperature is not taken into account because the experimental data include the data of thermal expansion strain by temperature.

During this drying process, nonlinear behavior (or softening behavior due to crack) of springs were observed. Iteration process is applied to re-distribute the forces around cracks.

3.3 Modeling of ITZ

Figure 6 shows constitutive law for ITZ in drying concrete in this simulation. As described in Chapter 1, ITZ is porous, and the strength and Young's modulus are lower than the mortar. Based on this fact, regarding the interface between aggregate and mortar, ITZ is modeled and the Young's modulus of ITZ is considered as 0.05 times of the aggregate. It should be noted that the ITZ part is strongly deteriorated after drying of concrete, because this part is restrained by the adjoining aggregate and many small cracks are yielded. Therefore, during the drying process, the ITZ is very soft. With regards to the fracture energy of ITZ, the report is scarce. Especially considering the very small region. Therefore, 0.1 times as much as that of mortar is applied. This fracture energy is relatively insensitive to the calculation results, but this value is determined by

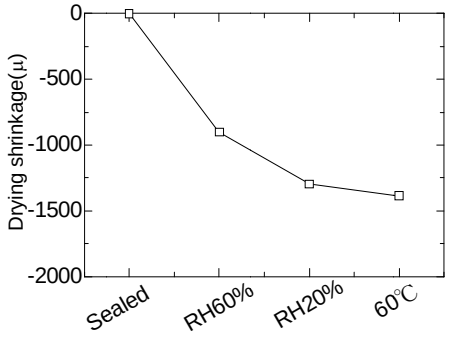

Fig. 5 Mortar drying shrinkage strain used for the calculations. Data are from ref. [11].

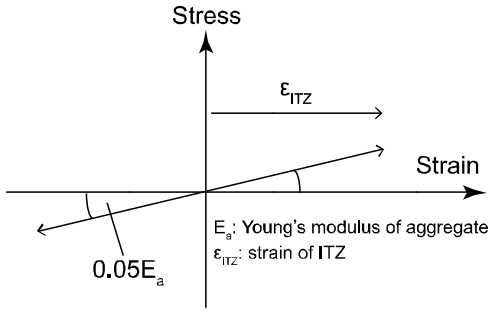

Fig. 6 Constitutive law for ITZ in drying concrete

the parametric study. Therefore, the parameters used here is the fitting parameters actually.

3.4 Analysis results

3.4.1 Cracking behavior under drying

Figure 7 shows calculated cracked surface in the specimen dried in 60% RH and 20 ºC, 20% RH and 20 ºC, and 60 ºC. To obtain this figure, averaged strain among the springs on the same surface is used. The averaged strain is defined by the following Eq(1),

$$\varepsilon_{face} = \sum_{N} \varepsilon_i \cdot A_{ii} / A_{face} \qquad (1)$$

where, ε_{face}: averaged Voronoi surface strain (μ), N:

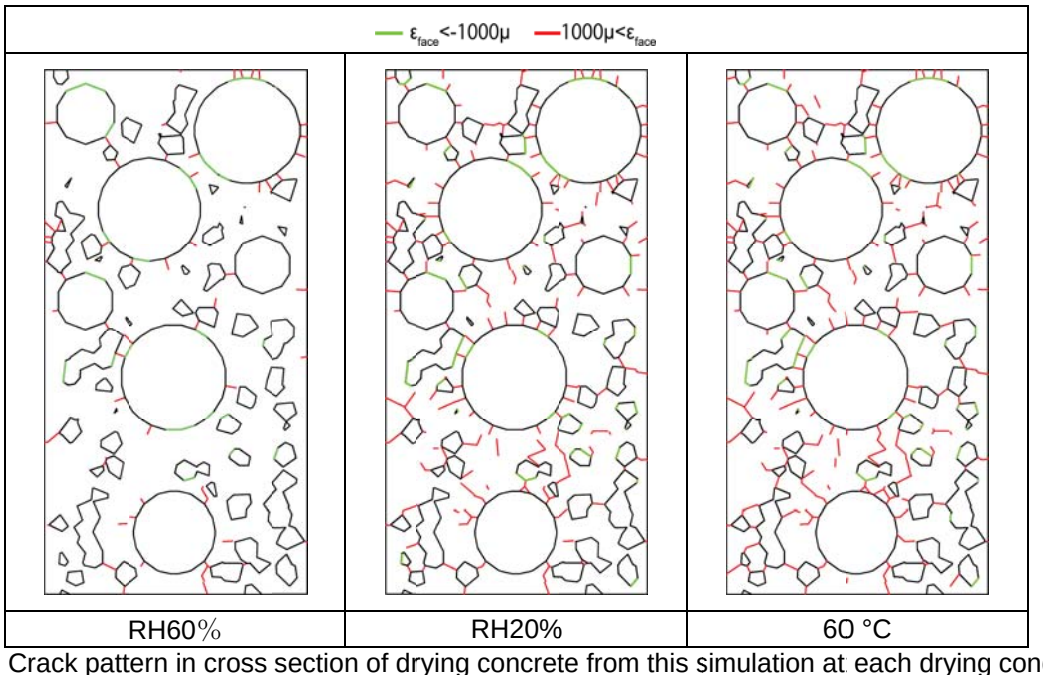

Fig. 7 Crack pattern in cross section of drying concrete from this simulation at each drying conditions

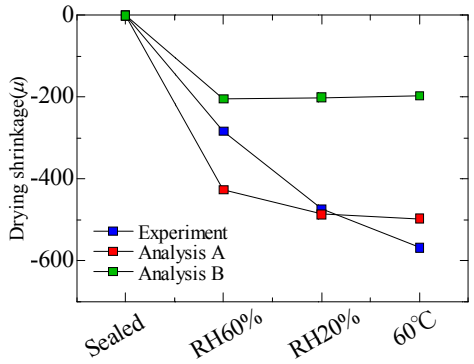

Fig. 8 Comparing drying shrinkage strain of this analysis and experiment

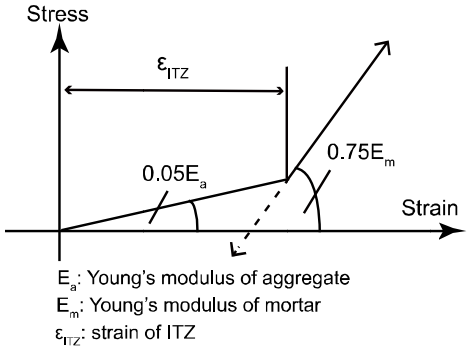

Fig. 9 Constitutive law for ITZ in concrete receiving compressive stress

number of springs on the Voronoi surface, A_i: area of triangle belongs to the spring (mm2), ε_i: strain of each spring (μ), A_{face}: the whole area of the Voronoi surface (mm2).

According to Fig. 7, at all drying condition, there are radial crack on the mortar around the aggregate. This is because, shrinkage of mortar is restrained by the aggregates, and resultantly, the tensile stress is yielded in the mortar around the aggregate. The stress in some part of mortar exceeded the strength and cracks were produced. This crack is propagated and connected the aggregates as the specimen is dried more intensely. This connecting cracks should have large impact on the strength of concrete. At the same time, like a ring test, surrounding mortar of the aggregates showed shrinking behavior, therefore, compression of some parts of surfaces was possible.

3.4.2 Shrinkage of concrete

Figure 8 shows the calculated results of drying shrinkage strains of the specimens with experimental data [11]. In this figure, the Young's modulus of ITZ in Analysis A is 0.05 times as much as that of the aggregate but in Analysis B is the same as that of mortar. After fitting the ITZ parameters, the shrinkage of concrete is reproduced satisfactory, while the shrinkage in results of Analysis B which did not consider the ITZ model is not. The proposed numerical calculation can provide the significant damage of aggregate scale under drying. And this process is almost consistent to our previous experimental results which were confirmed by digital image correlation method and fluor-epoxy resin impregnation method [12]. Through this calculation, it is found that it is necessary to take into account the ITZ for reproducing both damage in concrete and shrinkage strain under drying.

4. ANALYSIS OF UNAXIAL COMPRESSION TEST

4.1 Analysis method

After the drying process, simulation of uniaxial compression loading test was conducted for each specimen. As it is shown in Fig. 4, uniaxial compression test was simulated by locating the two rigid plates on the top and bottom surfaces of specimen, and these two rigid plates were compulsory moved. This process is by displacement control method and

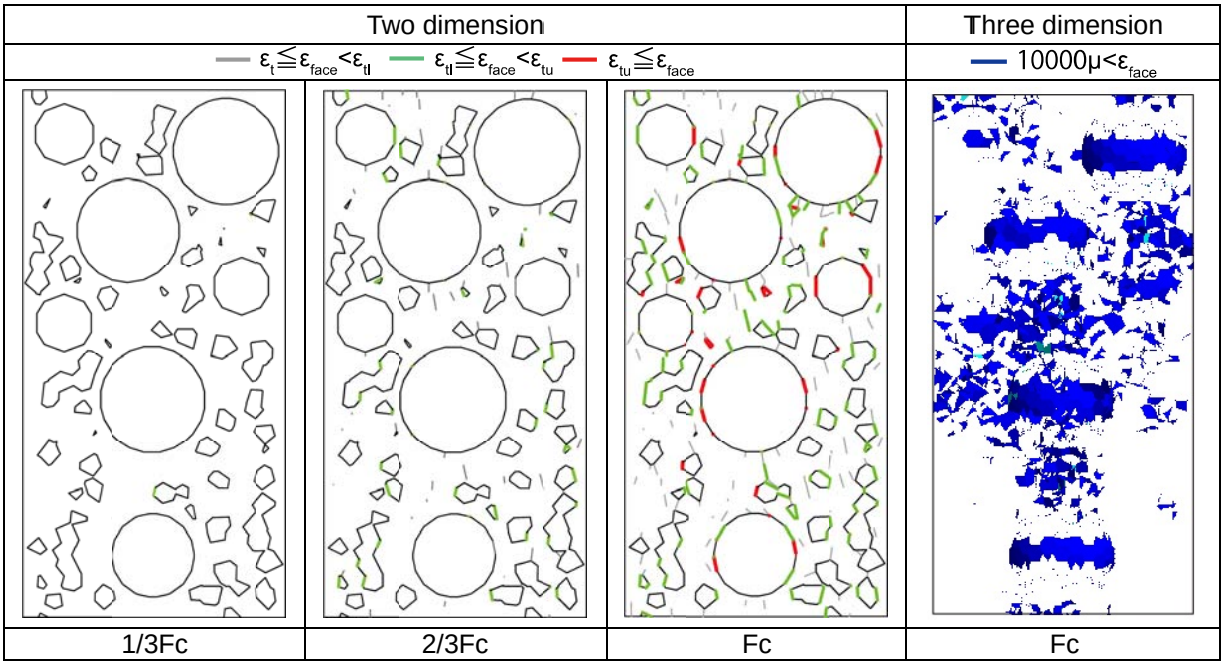

Fig. 10 Crack pattern in cross section of sealed concrete under compression stress from this simulation

incremental strain of the specimen was 10μ. The sealed condition, which is without drying process, is also conducted for the reference.

4.2 Modeling of ITZ

During the loading process, ITZ behavior is also very important, because the initiation of the crack under the loading process begins around coarse aggregate [13].

Consequently, the constitutive law for short term behavior of ITZ is proposed. In this model, the Young's modulus and tensile strength are assumed to be 0.75 times as large as that of mortar, and In addition, the fracture energy of ITZ is assumed to be 0.1 times as much as that of mortar. This is consistent to the long-term model of ITZ. The schematic of the proposed model is shown in Fig. 9.

4.3 Strength increase of cement paste

In the calculation process, the experimental fact that the mortar strength itself is affected by the drying process is taken into account. Because the hardened cement paste has a colloidal aspect, pore structure and atomic scale structure of calcium silicate hydrates are changed substantially under the first drying process. This colloidal behavior affects the strength of hardened cement paste [14]. Therefore, based on the experimental results [11, 14], strength of mortar was varied according to the drying conditions. In case of 20% RH condition, *Ft* is 2.0 times as large as that of sealed condition shown in Table 2, and in case of 60 ℃ condition, *Ft* is 3.0 times and *F*t is 1.1 times as much as that of sealed condition. In this analysis of uniaxial compression test, it was confirmed that the shear spring is fractured when the specimens of concrete is failed in compression. Thus, it is considered that the compressive strength of concrete specimens depends on the shear strength of the shear spring. On the contrary, few studies have been reported about the shear strength of dried concrete. Therefore, fitting experimental data,

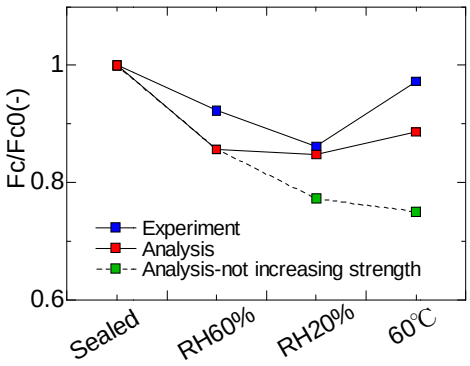

Fig. 11 Comparing ratio of compressive strength from this analysis and experiment

the value same as that of mortar is used. *C* and φ are 1.1 times as much as that of sealed condition

4.4 Analysis results

Figure 10 shows strain development of the normal springs corresponding to the tension stress. In this figure, strain of those springs is evaluated by Eq.(1) and the color zoning applied to this figure is same rules for the constitutive law for tension shown in Fig. 1. According to this figure, just before the maximum stress, vertical cracking besides aggregates are confirmed. In three dimensional figure, this trend is clearly observed. In addition, these cracks tend to connect each other. This process is consistent to the experimental observation [13]. From the reproducibility of failure process of concrete specimen under the uniaxial loading, the proposed ITZ model is feasible to this study.

Calculated results of ratio of compressive strength of dried specimens to that of the sealed condition are summarized in Fig. 11. In this figure, reference calculation results which did not take into account the mortar strength change due to drying are added. From this figure, it is clear that the damage in

concrete due to drying accumulated prior to the loading process has large impact on decrease in concrete strength. But in the experimental case, strength re-increase was shown, and this is explained by the strength change of cement paste due to drying. In general, calculation results which take into account the mortar strength change due to drying showed similar trend to that of experimental results.

However, absolute value of compressive strength is not completely reproduced here. It is suggested that impact of cracks are overestimated. For more precise evaluation, we have to take into account the water vapor transfer, resultant gradual drying, and alteration of mortar strength. This gradual changing may compensate the impact of cracks due to drying.

The significance of this calculation results is that the proposed numerical calculation procedure, which takes into account ITZ role in concrete, the mortar strength change originated from colloidal feature of calcium silicate hydrates, as well as damage in concrete derived from volumetric difference between coarse aggregate and mortar under the drying process, reflects the major mechanism of concrete strength alteration and shrinkage due to drying. The proposed calculation process reproduced the concrete behaviors of concrete strength and drying shrinkage strain at the same time.

5. CONCLUSIONS

In this study, drying shrinkage and uniaxial compression test of concrete are simulated by using rigid body spring network model. And ITZ behaviors are modeled for long-term drying processes and short-term loading. Considering these ITZ behaviors, shrinkage of concrete, strength alteration trend due to drying, damage accumulation due to volume change mismatch between mortar and coarse aggregates, were well reproduced.

The following points were shown in the calculation:

(1) Cracks in mortar around coarse aggregates under drying process were yielded and in severer drying cases those cracks tent to connect the aggregates.
(2) In analysis of drying shrinkage, modeling of ITZ is necessary to reproduce the concrete shrinkage, in which ITZ model takes into account the weak physical properties reflected by the porous characteristic.
(3) In analysis of uniaxial loading test, cracks, which along the coarse aggregates in parallel to the loading direction, are produced and number of cracks are increased and cracks tended to connect each other as the loading stress is increased.

These behaviors are also consistent to the previous experimental researches.

ACKNOWLEDGEMENT

A part of present study are sponsored by JSPS KAKENHI Grant Number 15H04077.

REFERENCES

[1] Architectural Instituite of Japan, Guidelines for Maintenance and Management of Structures in Nuclear Facilities, Maruzen, 2015.
[2] A. Sugie, I. Maruyama, and M. Teshigawara, “Numerical simulation for stiffness change of RC wall due to drying, Summaries of technical papers of annual meeting,” vol.A, 2014, pp.1175-1176.
[3] Jianzhuang Xiao et al, “Properties of interfacial transition zone in recycled aggregate concrete tested by nanoindentation,” Cement and Concrete Composites, Vol.37, 2013, pp. 276-292.
[4] J.P.Olivier, J.C.Maso, and B.Bourdette, “Interfacial transition zone in concrete,” Advanced Cement Based Materials, Vol.2, No.1, 1995, pp.30-38.
[5] R.Zimbelmann, “A method for strengthening the bond between cement stone and aggregates,” Cement and Concrete Research, Vol.17, pp. 651-660.
[6] H. Uchikawa, “Influence of Interfacial Structure between Cement Paste and Aggregate on the Quality of Hardened Concrete,” Concrete journal , Vol. 33, No. 9, 1995, pp. 5-17.
[7] H. S. Wong et al, “Influence of the interfacial transition zone and microcracking on the diffusivity, permeability and sorptivity of cement-based materials after drying,” Magazine of Concrete Research Vol. 61, No. 8, 2009, pp. 571-589.
[8] I. Maruyama, A. Sugie, “Numerical Study on Drying Shrinkage of Concrete Affected by Aggregate Size,” Journal of Advanced Concrete Technology, Vol. 12, No. 8, 2014, pp. 279-288.
[9] X. Ping and J. J. Beaudoin,” Effects of transition zone microstructure on bond strength of aggregate-portland cement paste interfaces,” Cement and Concrete Research, Vol. 22, No. 1, 1992, pp. 23-26.
[10] Y.Yamamoto, “Analysis of compression failure of concrete by three dimensional rigid body spring model , ” Journal of Japan society of civil engiberrs E, Vol. 64,.No. 4, 2008, pp. 612-630.
[11] I. Maruyama et. al, “Strength and Young’s modulus change in concreate due to long-term drying heating up to 90°C,” Cement and Concrete Research Vol. 66, 2014, pp. 48-63.
[12] I. Maruyama and H. Sasano, “Strain and crack distribution in concrete during drying,” Mater Struct Vol. 47, No. 3, 2014, pp. 517-532.
[13] S. Choi, S.P. Shah,” Propagation of Micro cracks in Concrete Studied with Subregion Scanning Computer Vision (SSCV),” ACI Materials Journal, Vol. 96, 1999, pp. 255-260.
[14] I. Maruyama et al, “Microstructure and bulk property changes in hardend cement past during the first drying process,” Cement and Concrete Research Vol. 58, 2014, pp.20-34